

## Supporting Information for

# A Visible Light Water-Splitting Cell with a Photoanode formed by Codeposition of a High-Potential Porphyrin and an Iridium Water-Oxidation Catalyst

Gary F. Moore, James D. Blakemore, Rebecca L. Milot, Jonathan F. Hull, Hee-eun Song, Lawrence Cai, Charles A. Schmuttenmaer,\* Robert H. Crabtree,\* and Gary W. Brudvig\*

Department of Chemistry, Yale University, P.O. Box 208107, New Haven, Connecticut 06520-8107

E-mail: [g.moore@yale.edu](mailto:g.moore@yale.edu), [charles.schmuttenmaer@yale.edu](mailto:charles.schmuttenmaer@yale.edu), [robert.crabtree@yale.edu](mailto:robert.crabtree@yale.edu),  
[gary.brudvig@yale.edu](mailto:gary.brudvig@yale.edu)

<i>Index</i>	<i>Page</i>
<b>S1. Experimental Procedures</b>	<b>S2-S3</b>
<b>S2. Synthesis and Structural Characterization</b>	<b>S4-S7</b>
<b>S3. Nuclear Magnetic Resonance Spectra</b>	<b>S7-S9</b>
<b>S4. Optical and Electrochemical Data</b>	<b>S7-S12</b>
<b>S5. X-ray Crystal Structure of Cp*IrCl(3'-carboxy-2-phenylpyridine)</b>	<b>S12-S16</b>
<b>S.6. References</b>	<b>S17</b>

## S1. Experimental Procedures

All reagents were purchased from Aldrich, Alfa Aesar or Mallinckrodt. Dichloromethane was purified with a solvent purification system (Innovative Technologies, Inc) using a 1-m column containing activated alumina. All solvents were stored over the appropriate molecular sieves prior to use. MilliQ water was used to prepare all of the aqueous solutions.

### S1.1. Sample preparation and characterization

All compounds were synthesized from commercially available starting materials (see SI, Synthesis and Structural Characterization). Thin layer chromatography (TLC) was performed with silica gel coated glass plates from EMD Chemicals. Column chromatography was carried out using silica gel 60, 230-400 mesh from EMD Chemicals. NMR spectra were recorded on Bruker spectrometers operating at 400 or 500 MHz. NMR samples were prepared in deuteriochloroform or 1% deuteriopyridine in deuteriochloroform with tetramethylsilane as an internal reference for  $^1\text{H}$ -NMR and trichlorofluoromethane as an external reference for  $^{19}\text{F}$ -NMR. Mass spectra were obtained with a matrix-assisted laser desorption/ionization time-of-flight spectrometer (MALDI-TOF). Steady-state absorbance spectra were measured on a Varian Cary 300 UV-visible spectrophotometer. Steady-state fluorescence spectra were measured using a Shimadzu RF-5301PC spectrometer.

Photoanodes were prepared in a manner similar to that reported previously.<sup>1</sup> Commercially available P25  $\text{TiO}_2$  nanoparticles were used as received from Degussa (now Evonik). Fluorine-doped tin oxide (FTO) conductive glass slides (Tec 8, visible light transmittance 77 %, Hartford Inc., USA) were rinsed with ethanol before use. Pastes composed of 1.0 g  $\text{TiO}_2$  in 2 mL Milli-Q water were stirred overnight to obtain a homogeneous dispersion and then coated by the doctor-blade method onto the FTO glass slides with area 1 to 1.3  $\text{cm}^2$  and thickness  $\sim 10 \mu\text{m}$ . The electrodes were dried at room temperature and sintered in air at 450  $^\circ\text{C}$  for 2 h with a ramp rate 5  $^\circ\text{C}/\text{min}$ . The  $\text{TiO}_2$  electrodes were sensitized by soaking the slide in a 0.1 mM solution of porphyrin compound **1**, catalyst compound **2**, or a 1:1 mixture of **1** and **2** (each 0.1 mM in concentration) in 10% ethanol in dichloromethane overnight at room temperature. Following sensitization, the photoanodes were rinsed with 10% ethanol in dichloromethane solution and dried at room temperature.

### S1.2 Electrochemical measurements

Cyclic voltammetry was performed with an EG&G Princeton Applied Research Model 273A potentiostat/galvanostat using a glassy carbon (3 mm diameter) or platinum disc (1.6 mm diameter) or FTO working electrode, a platinum counter electrode, and a silver wire pseudoreference electrode or a Ag/AgCl electrode (Bioanalytical Systems, Inc. Ag/AgCl vs. NHE: +197 mV)<sup>2, 3</sup> in a conventional three-electrode cell. For organic solutions, anhydrous dichloromethane or acetonitrile was used as the solvent. The supporting electrolyte was 0.10 M tetrabutylammonium perchlorate or 0.10 M tetrabutylammonium hexafluorophosphate and the solution was deoxygenated by bubbling with nitrogen. The platinum disc working electrode was cleaned between experiments by polishing with an alumina slurry, followed by solvent rinses. The concentration of the electroactive compound was  $\sim 3 \times 10^{-3}$  M. The potential of the pseudoreference electrode was determined using the ferrocenium/ferrocene redox couple as an internal standard (with  $E_{1/2}$  taken as 0.690 V vs. NHE in dichloromethane).<sup>2</sup> For aqueous solutions, the supporting electrolyte was 0.1 M  $\text{Na}_2\text{SO}_4$ . All reported voltammograms were

recorded at a  $100 \text{ mV s}^{-1}$  scan rate. All potentials listed in this manuscript are referenced to the normal hydrogen electrode (NHE) unless otherwise stated.

Aqueous rotating ring-disc electrochemistry (RRDE) experiments were carried out with a Pine AFCBP1 Bipotentiostat and a Pine MSR variable-speed rotator. The supporting electrolyte was  $0.1 \text{ M Na}_2\text{SO}_4$ . The reference was a Ag/AgCl electrode (Bioanalytical Systems, Inc., Ag/AgCl vs. NHE:  $+197 \text{ mV}$ )<sup>2, 3</sup> and the counter electrode was a platinum wire. The disc and ring electrode materials were platinum. The platinum disc was prepared with a  $\text{TiO}_2$  film in the manner described above by doctor blading and sintering.

### S1.1.3. Elemental analysis

All samples were analyzed on a Costech ECS 4010 elemental analyzer (Costech Analytical Technologies, Valencia, CA) coupled to a ThermoFinnigan DeltaPLUS Advantage stable isotope mass spectrometer (Thermo Scientific, Boca Raton, FL), with both controlled by the Thermo's Isodat 2.0 software. In a typical run, a dried  $\text{TiO}_2$  sample (0.5–1.0 mg) was sealed in a tin capsule and loaded into the autosampler. Control experiments were run using pure  $\text{TiO}_2$  materials and powdered complex **1**, and the results were calibrated with the house standard (standard cocoa powder, 4.15% N; 48.7% C). The output of the elemental analyzer, the  $\text{N}_2$  and the  $\text{CO}_2$  from N and C on  $\text{TiO}_2$  surfaces, was sampled by the mass spectrometer.

### S1.4. Reflectance measurements

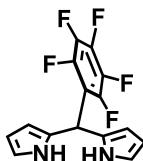
UV/visible spectra were taken on a Varian Cary 300 spectrophotometer with an integrating sphere attachment. Thin films of  $\text{TiO}_2$  samples were doctor-bladed on microscope slides and heated to  $450 \text{ }^\circ\text{C}$  for 2 h with a ramp rate of  $5 \text{ }^\circ\text{C}/\text{min}$ . The thin films were then sensitized with porphyrin dye **1** and/or catalyst **2** by soaking in a 10% solution of ethanol in dichloromethane overnight and dried at room temperature before collecting spectra. The same sensitized films were also used in the THz studies.

### S1.5. Time-resolved terahertz spectroscopy measurements

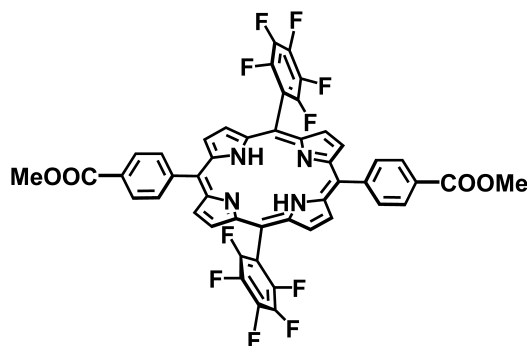
Interfacial electron-transfer dynamics of functionalized metal-oxide nanoparticle thin films were studied, with subpicosecond temporal resolution, using time-resolved terahertz spectroscopy. In these experiments, THz radiation is absorbed by mobile electrons in the metal-oxide conduction band, and the change in THz amplitude is a product of the carrier density and mobility.<sup>4, 5</sup> Photoexcitation and subsequent electron injection results in an increase of the metal-oxide free-carrier population, decreasing the THz transmission amplitude. Such measurements allow for a direct comparison of the timescale and efficiency of photoinduced charge injection and recombination or trapping. An amplified Ti:sapphire laser (Tsunami/Spitfire from Spectra Physics) generated 800 mW of pulsed near-IR light at a 1 kHz repetition rate. The pulse width was 100 fs, and the center wavelength was 800 nm. Roughly two-thirds of the power was frequency doubled and then filtered to produce 40 mW of 400 nm (3.10 eV) light for the pump beam. The remainder of the near-IR light was used to generate and detect THz radiation. Terahertz radiation was generated using optical rectification in a ZnTe(110) crystal and detected using free-space electro-optic sampling in a second ZnTe (110) crystal. Terahertz data were taken at room temperature using the samples that were prepared for UV/visible measurements, and the average of two samples was taken for each data set. To analyze electron injection

dynamics, the change in THz transmission was monitored as the time delay between the 400-nm pump pulse and the THz probe pulse was varied. Further information on the spectrometer and techniques is reported in the literature.<sup>4,6</sup>

## S2. Synthesis and Characterization:

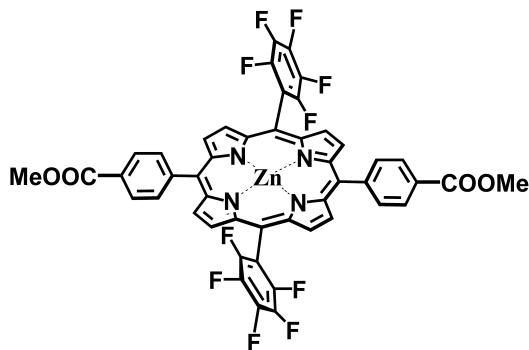


**5-(Pentafluorophenyl)dipyrromethane.** A similar method was previously reported.<sup>7</sup> A solution of pentafluorobenzaldehyde (2.0 mL, 16.2 mmol) in freshly distilled pyrrole (50 mL, 720 mmol) was degassed with a stream of argon for 20 min before adding trifluoroacetic acid (120  $\mu$ L, 1.62 mmol). The mixture was stirred for 30 min at room temperature, diluted with  $\text{CH}_2\text{Cl}_2$  (400 mL), and then washed with 0.1M NaOH (400 mL). The organic phase was washed with water (400 mL) and dried over  $\text{Na}_2\text{SO}_4$ . Evaporation of the solvent at reduced pressure gave brown oil. Unreacted pyrrole was removed under high vacuum, yielding a tacky solid that was flashed on a column of silica using a mixture of hexanes:ethyl acetate:triethylamine (80:20:1) as the eluent. The product was recrystallized from dichloromethane/hexanes to yield 3.29 g of 5-(pentafluorophenyl)dipyrromethane as a white powder (65% yield).  $^1\text{H}$  NMR (400 MHz,  $\text{CDCl}_3$ ):  $\delta$  5.90 (1H, s, CH), 6.00 – 6.05 (2H, m, ArH), 6.14– 6.19 (2H, m, ArH), 6.71 – 6.75 (2H, m, ArH), 8.06 (2H, brs, NH);  $^{19}\text{F}$  NMR (400 MHz,  $\text{CDCl}_3$ ):  $\delta$  -160.98 – -161.40 (2F, m, ArF), -155.71 (1F, t,  $J = 21.0$  Hz, ArF), -141.43 (2F, brd,  $J = 20.7$  Hz, ArF).



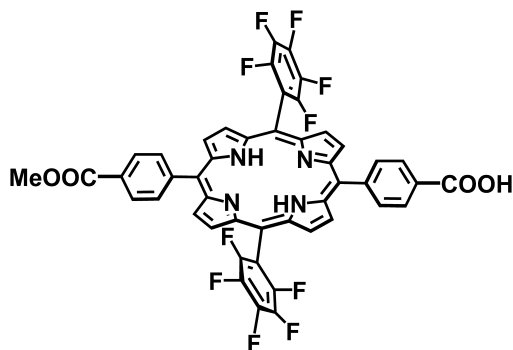
**5,15-Bis(4-carbomethoxyphenyl)-10,20-bis(pentafluorophenyl)porphyrin.** A portion of 5-(pentafluorophenyl)dipyrromethane (1.15 g, 3.68 mmol), and 4-carbomethoxybenzaldehyde (663 mg, 3.68 mmol) in chloroform (370 mL) was purged for 20 minutes with argon before adding  $\text{BF}_3(\text{OEt}_2)$  (486  $\mu$ L of a 2.5M stock solution in chloroform). After 24 h, 2,3-dichloro-5,6-dicyano-1,4-benzoquinone (DDQ) (625 mg, 2.75 mmol) was added and the mixture was stirred for an additional 24 h. The solvent was evaporated at reduced pressure and the residue was redissolved in toluene. The solution was treated with a second portion of DDQ (625 mg, 2.75 mmol) and refluxed for 2.5 h. The toluene was removed at reduced pressure and the crude product was purified by column chromatography on silica using chloroform as the eluent. Recrystallization from chloroform/methanol gave 318 mg of the desired porphyrin as a purple

crystalline solid (19% yield).  $^1\text{H}$  NMR (400 MHz,  $\text{CDCl}_3$ ):  $\delta$  -2.86 (2H, s, NH), 4.13 (6H, s,  $\text{CO}_2\text{CH}_3$ ), 8.31 (4H, d,  $J = 8.1$  Hz, ArH), 8.47 (4H, d,  $J = 8.1$  Hz, ArH), 8.83 (4H, d,  $J = 4.8$  Hz,  $\beta\text{H}$ ), 8.91 (4H, d,  $J = 4.8$  Hz,  $\beta\text{H}$ );  $^{19}\text{F}$  NMR (400 MHz, in  $\text{CDCl}_3$ ):  $\delta$  -161.49 – -161.96 (4F, m, ArF), -151.95 (2F, t,  $J = 21.2$  Hz, ArF); -136.81 (4F, dd,  $J = 8.1$  Hz, 23.7 Hz, ArF); MALDI-TOF-MS  $m/z$ . calcd. for  $\text{C}_{48}\text{H}_{24}\text{F}_{10}\text{N}_6\text{O}_4$  910.164, obsd. 910.169; UV-vis ( $\text{CH}_2\text{Cl}_2$ ) 416, 510, 543 587, 641 nm. Emission ( $\text{CH}_2\text{Cl}_2$ ) 646, 709 nm.



**Zinc 5,15-bis(4-carbomethoxyphenyl)-10,20-bis(pentafluorophenyl)porphyrin.**

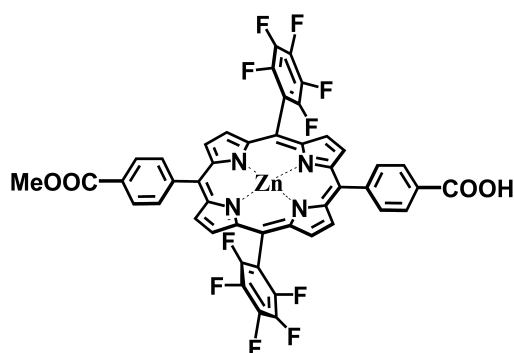
$\text{Zn}(\text{OAc})_2 \cdot 2\text{H}_2\text{O}$  (84 mg, 0.38 mmol) was added to a solution of 5,15-bis(4-carbomethoxyphenyl)-10,20-bis(pentafluorophenyl)porphyrin (35 mg, 0.04 mmol) in a mixture of dichloromethane and methanol (80:20, 50 mL). After stirring for 15 h, the solution was diluted with dichloromethane (25 mL) and washed with water (75 mL), then a saturated solution of aqueous sodium bicarbonate. The organic phase was dried over sodium sulfate, filtered, and the solvent evaporated at reduced pressure. The product was purified by column chromatography on silica using dichloromethane as the eluent to give 37 mg of the desired porphyrin (98% yield).  $^1\text{H}$  NMR (500 MHz, 1% Pyridine- $d_5$  in  $\text{CDCl}_3$ ):  $\delta$  4.09 (6H, s,  $\text{CO}_2\text{CH}_3$ ), 8.24 (4H, d,  $J = 8.3$  Hz, ArH), 8.42 (4H, d,  $J = 8.3$  Hz, ArH), 8.87 (4H, d,  $J = 4.8$  Hz,  $\beta\text{H}$ ), 8.90 (4H, d,  $J = 4.8$  Hz,  $\beta\text{H}$ );  $^{19}\text{F}$  NMR (400 MHz, 1% Pyridine- $d_5$  in  $\text{CDCl}_3$ ):  $\delta$  -162.68 – -162.49 (4F, m, ArF), -153.29 (2F, t,  $J = 20.9$  Hz, ArF); -137.54 (4F, dd,  $J = 8.5$  Hz, 24.7 Hz, ArF); MALDI-TOF-MS  $m/z$ . calcd. for  $\text{C}_{48}\text{H}_{22}\text{F}_{10}\text{N}_6\text{O}_4\text{Zn}$  927.077, obsd. 927.079 UV-vis ( $\text{CH}_2\text{Cl}_2$ ) 415, 545, 578 nm Emission ( $\text{CH}_2\text{Cl}_2$ ) 590, 642 nm.



**5-(4-Carbomethoxyphenyl)-15-(4-carboxyphenyl)-10,20-bis(pentafluorophenyl)porphyrin.**

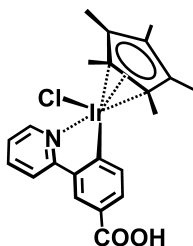
A portion of 5,15-bis(4-carbomethoxyphenyl)-10,20-bis(pentafluorophenyl)porphyrin (100 mg, 0.11 mmol) was dissolved in a mixture of trifluoroacetic acid and conc. HCl (1:2, 80 mL) at 45 $^\circ$

C for 24 h. The reaction mixture was diluted with dichloromethane (80 mL), washed twice with an equal volume of water, and then neutralized with a saturated solution of aqueous sodium bicarbonate. The organic phase was dried over sodium sulfate, filtered, and the solvent removed at reduced pressure. The crude product was purified by column chromatography on silica using a gradient of 1% methanol in dichloromethane to 10% methanol in dichloromethane as the eluent to give 59 mg of the desired porphyrin (60% yield).  $^1\text{H}$  NMR (500 MHz, 1% Pyridine-*d*5 in  $\text{CDCl}_3$ ):  $\delta$  -2.86 (2H, s, NH), 4.11 (3H, s,  $\text{CO}_2\text{CH}_3$ ), 8.30 (2H, d,  $J = 8.4$  Hz, ArH), 8.31 (2H, d,  $J = 8.4$  Hz, ArH), 8.48 (2H, d,  $J = 8.2$  Hz, ArH), 8.59 (2H, d,  $J = 8.2$  Hz, ArH), 8.87 (4H, brm,  $\beta\text{H}$ ), 8.91 (2H, d,  $J = 4.8$  Hz,  $\beta\text{H}$ ), 8.96 (2H, d,  $J = 4.8$  Hz,  $\beta\text{H}$ );  $^{19}\text{F}$  NMR (400 MHz, 1% Pyridine-*d*5 in  $\text{CDCl}_3$ ):  $\delta$  -161.96 – -161.78 (4F, m, ArF), -152.16 (2F, t,  $J = 21.0$  ArF), -137.03 (4F, dd,  $J = 8.0$  Hz, 23.9 Hz, ArF); MALDI-TOF-MS  $m/z$ . calcd. for  $\text{C}_{47}\text{H}_{22}\text{F}_{10}\text{N}_4\text{O}_4$  896.148, obsd. 896.153.



**Zinc 5-(4-carbomethoxyphenyl)-15-(4-carboxyphenyl)-10,20-bis(pentafluorophenyl)**

**porphyrin (1).**  $\text{Zn}(\text{OAc}_2) \cdot 2\text{H}_2\text{O}$  (98 mg, 0.45 mmol) was added to a solution of 5-(4-carbomethoxyphenyl)-15-(4-carboxyphenyl)-10,20-bis(pentafluorophenyl)porphyrin (40 mg, 0.04 mmol) in a mixture of dichloromethane and methanol (80:20, 60 mL). After stirring for 15 h, the solution was diluted with dichloromethane (25 mL) and washed with water (85 mL), then a saturated solution of aqueous sodium bicarbonate. The organic phase was dried over sodium sulfate, filtered, and the solvent evaporated at reduced pressure. The product was purified by column chromatography on silica using 5% methanol in dichloromethane as the eluent to give 42 mg of the desired porphyrin (97% yield).  $^1\text{H}$  NMR (500 MHz, 1% Pyridine-*d*5 in  $\text{CDCl}_3$ ):  $\delta$  4.10 (3H, s,  $\text{CO}_2\text{CH}_3$ ), 8.24 (2H, d,  $J = 8.1$  Hz, ArH), 8.25 (2H, d,  $J = 8.1$  Hz, ArH), 8.42 (2H, d,  $J = 8.1$  Hz, ArH), 8.52 (2H, d,  $J = 8.1$  Hz, ArH), 8.87 (4H, brd,  $J = 4.6$  Hz,  $\beta\text{H}$ ), 8.90 (2H, d,  $J = 4.6$  Hz,  $\beta\text{H}$ ); 8.95 (2H, d,  $J = 4.6$  Hz,  $\beta\text{H}$ );  $^{19}\text{F}$  NMR (400 MHz, 1% Pyridine-*d*5 in  $\text{CDCl}_3$ ):  $\delta$  -162.76 – -162.51 (4F, m, ArF), -153.37 (2F, t,  $J = 21.1$  Hz, ArF); -137.51 (4F, dd,  $J = 8.3$  Hz, 24.5 Hz, ArF); MALDI-TOF-MS  $m/z$ . calcd. for  $\text{C}_{47}\text{H}_{20}\text{F}_{10}\text{N}_4\text{O}_4\text{Zn}$  958.062, obsd. 958.062.



**Cp\*IrCl(3'-carboxy-2-phenylpyridine) (2).** A solution of [Cp\*IrCl<sub>2</sub>]<sub>2</sub> (300 mg, 0.38 mmol) in dichloromethane (10 mL) was added to a mixture of 3-(pyridin-2-yl)benzoic acid (150 mg, 0.75 mmol) and NaOAc•3H<sub>2</sub>O (132 mg, 0.97 mmol) in methanol (10 mL). The mixture was purged with argon, stirred at room temperature for 24 h, filtered twice through celite and the solvent evaporated at reduced pressure. The product was purified by recrystallization from dichloromethane/hexanes (174 mg, 40 % yield). <sup>1</sup>H NMR (500 MHz, CDCl<sub>3</sub>): δ 1.62 (15H, s, CH<sub>3</sub>), 7.10-7.14 (1H, m, PyrH), 7.66-7.71 (1H, m, PyrH), 7.78 (1H, d, *J* = 7.9 Hz, ArH), 7.85 (1H, d, *J* = 7.9 Hz, ArH), 7.92 (1H, d, *J* = 7.9 Hz, PyrH), 8.31 (1H, s, ArH); 8.66 (1H, d, *J* = 5.7 Hz, PyrH).

### S3. Nuclear Magnetic Resonance Spectra:

**Figure S1.** 500 MHz <sup>1</sup>H NMR spectra and overlaid COSY of 5-(4-carbomethoxyphenyl)-15-(4-carboxyphenyl)-10,20-bis(pentafluorophenyl)porphyrin recorded in 1 % pyridine-*d*<sub>5</sub> in chloroform-*d*.

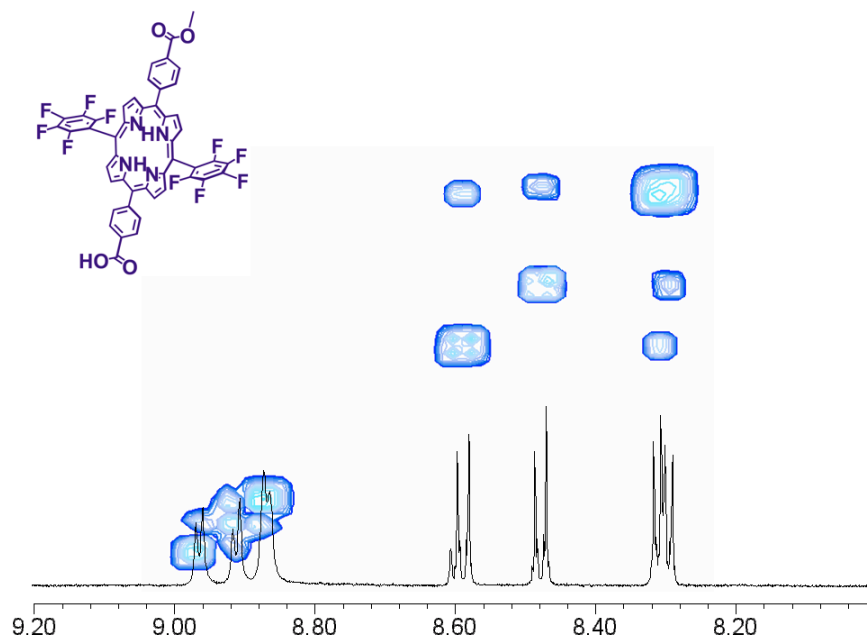


**Figure S2.** 500 MHz  $^1\text{H}$  NMR spectra and overlaid COSY of **1** recorded in 1 % pyridine-*d*5 in chloroform-*d*.

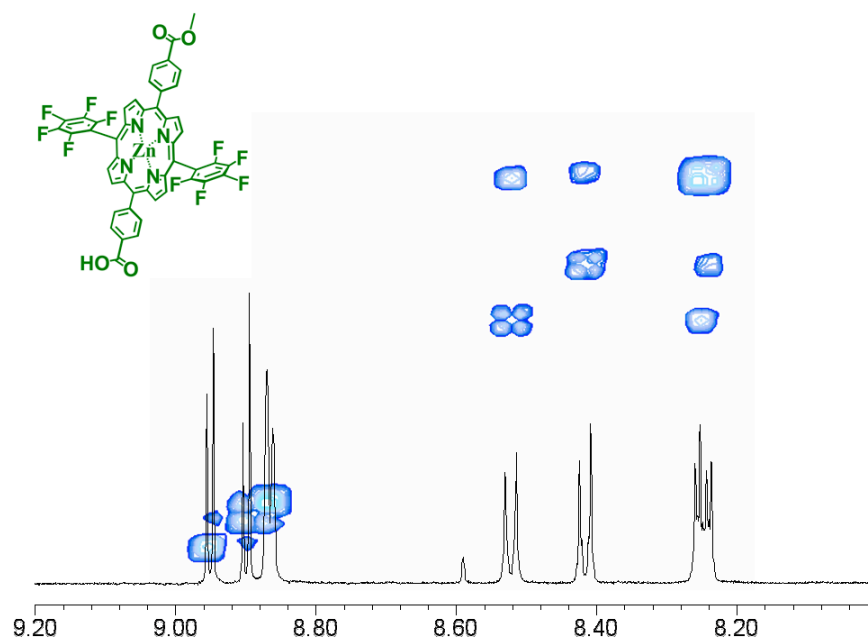


**Figure S3.** 400 MHz  $^{19}\text{F}$  NMR spectra of **1** recorded in 1 % pyridine-*d*5 in chloroform-*d*.

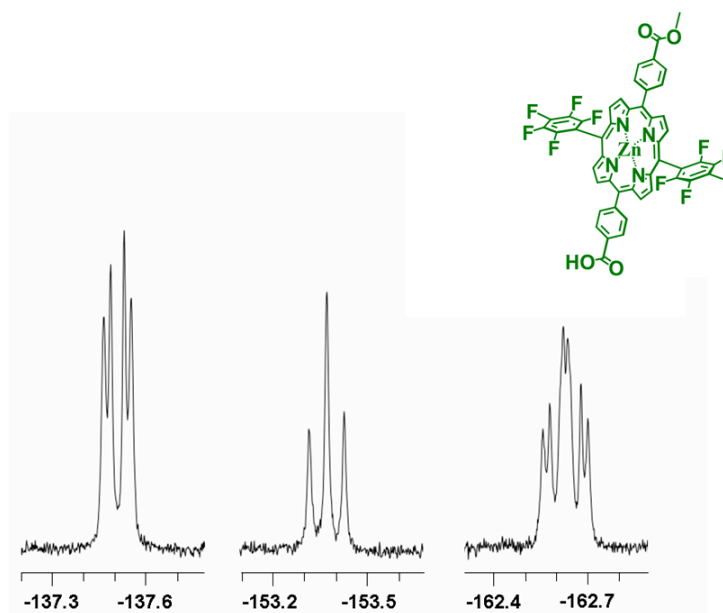
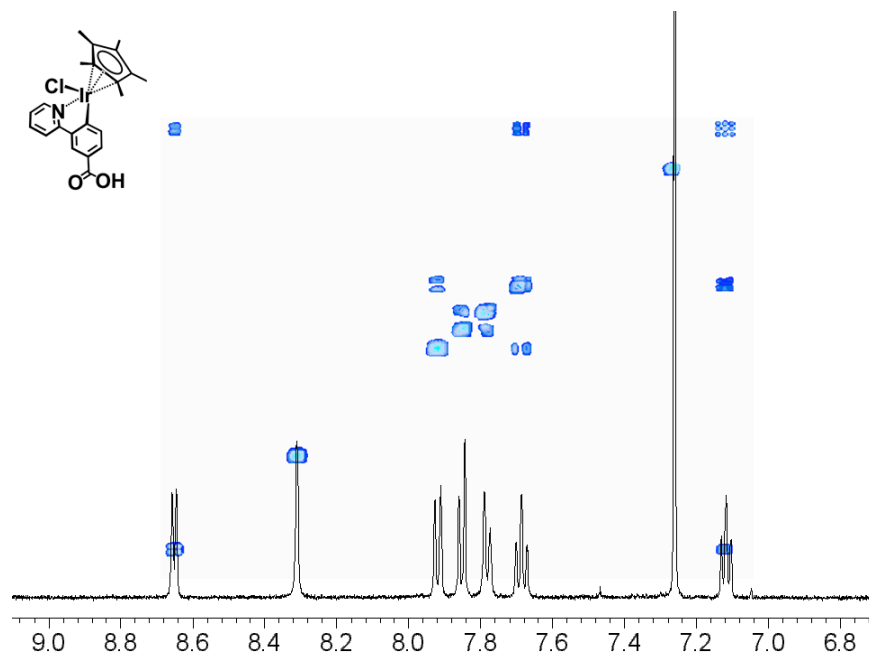


**Figure S4.** 500 MHz  $^1\text{H}$  NMR spectra and overlaid COSY of **2** recorded in chloroform-*d*.



#### S4. Optical and Electrochemical Data:

**Figure S5.** Cyclic voltammogram (left) recorded at a glassy carbon electrode as well as the absorption spectrum (right), of 5,15-Bis(4-carbomethoxyphenyl)-10,20-bis(pentafluorophenyl) porphyrin in dichloromethane.

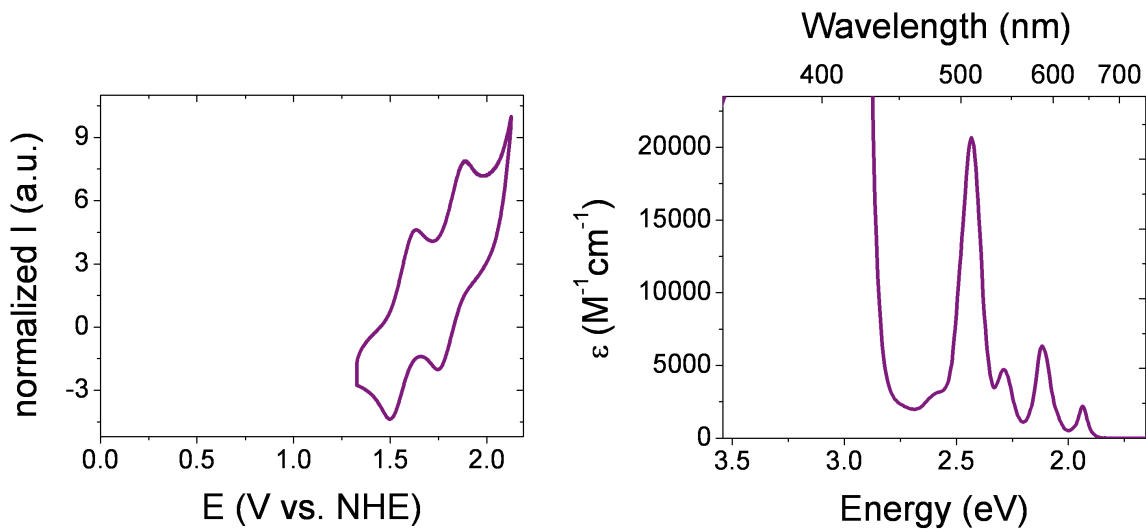


**Figure S6.** Normalized absorption (solid) and emission (left) spectra of 5,15-Bis(4-carbomethoxyphenyl)-10,20-bis(pentafluorophenyl) porphyrin recorded in dichloromethane, showing the overall spectral profiles (left) as well the intersection of the normalized longest-wavelength absorption and shortest-wavelength emission band, giving an estimated  $E^{0-0}$  transition energy of  $\sim 1.93$  eV.

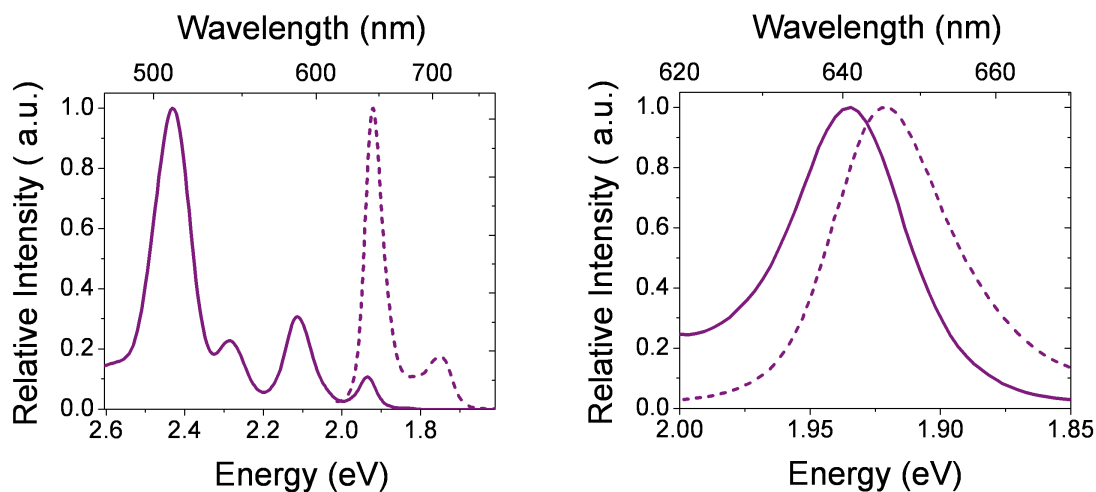


**Figure S7.** Cyclic voltammograms (left) recorded at a glassy carbon electrode in a dichloromethane solution of the methyl ester of zinc porphyrin **1** (green) and an acetonitrile solution of our unfunctionalized iridium catalyst (black) as well as absorption spectra (right), recorded in a dichloromethane of the methyl ester of zinc porphyrin **1** (green) and the iridium catalyst **2** (black).

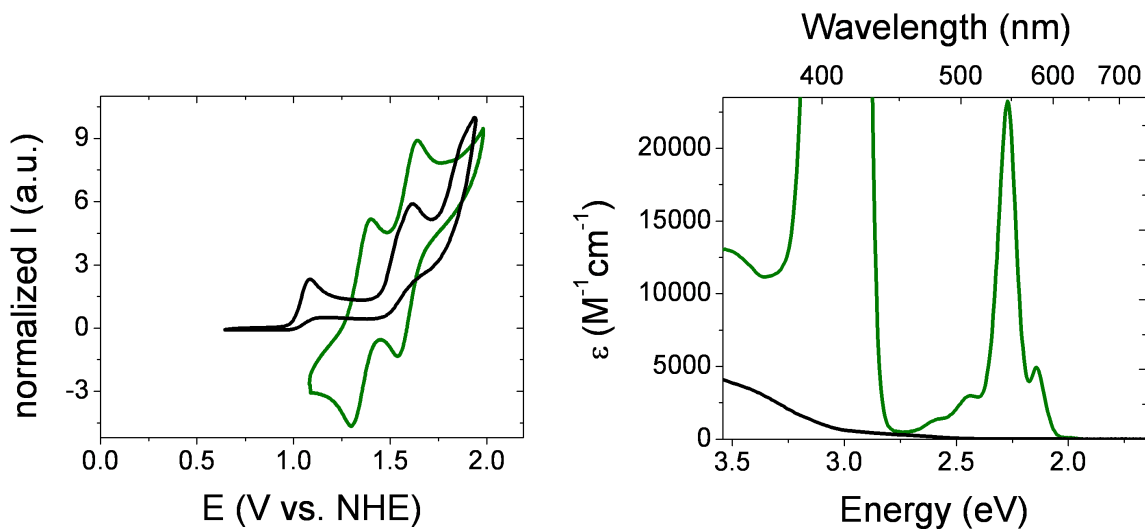


**Figure S8.** Normalized absorption (solid) and emission (left) spectra of the methyl ester of zinc porphyrin **1** recorded in dichloromethane, showing the overall spectral profiles (left) as well the intersection of the normalized longest-wavelength absorption and shortest-wavelength emission band, giving an estimated  $E^{0-0}$  transition energy of  $\sim 2.12$  eV.

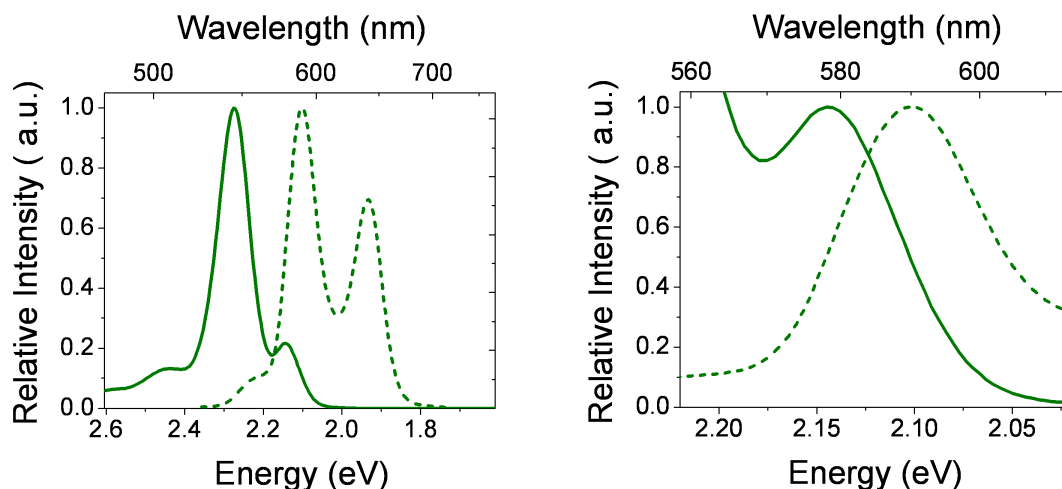


**Figure S9.** Normalized absorption (green) of the methyl ester of zinc porphyrin **1** recorded in dichloromethane and the diffuse reflectance spectra (dark yellow) of **1-TiO<sub>2</sub>** (illustrated in green in Figure 1 of the manuscript). The reflectance spectrum of the immobilized species appears bathochromically shifted in comparison with solution absorption measurements of the model compound, indicating a coupling of the transition moments of the constituent dyes on the surface consistent with J-aggregation.

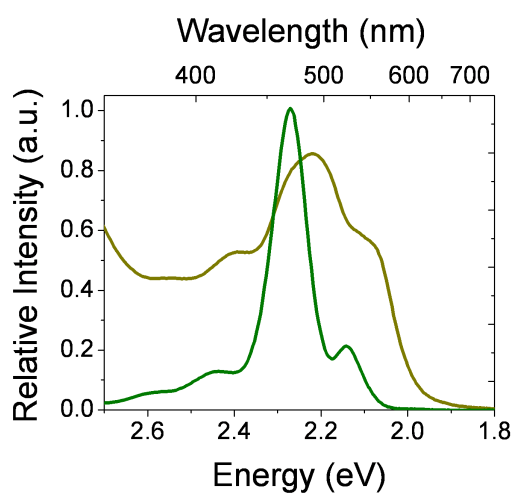
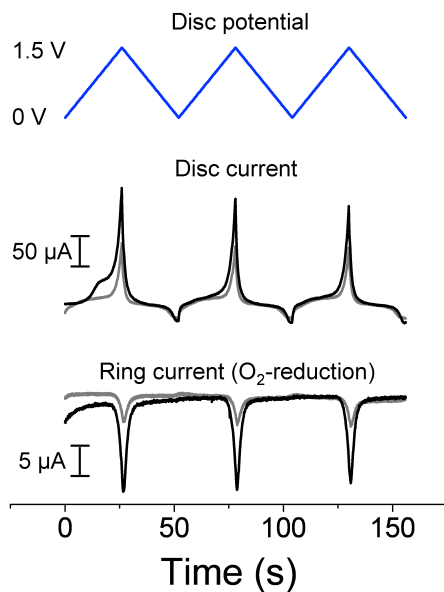
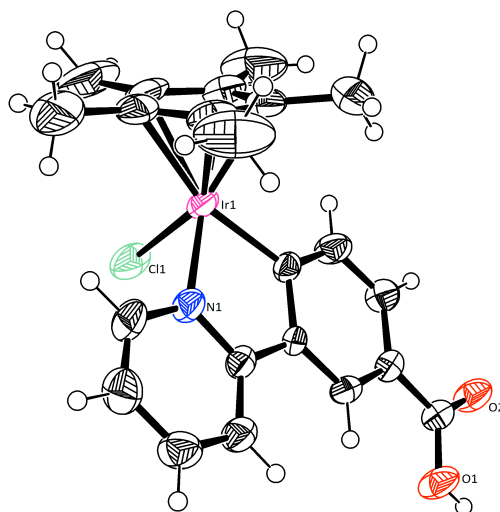


**Figure S10.** Rotating ring-disk electrode measurements (100 mV/s) of oxygen evolution from a 0.1 M  $\text{Na}_2\text{O}_4$  aqueous solution using a  $\text{TiO}_2$  sintered Pt-disk electrode (grey) and 2-functionalized  $\text{TiO}_2$  sintered Pt-disk electrode (black). (top) Disc potential. (middle) Disc current. (bottom) Pt-ring current. (The Pt-ring was held at -0.3 V vs. NHE.)



### S5. X-ray Crystal Structure of $\text{Cp}^*\text{IrCl}(3'$ -carboxy-2-phenylpyridine) (2):

**Figure S11.** X-ray crystal structure of  $\text{Cp}^*\text{IrCl}(3'$ -carboxy-2-phenylpyridine) (2)



### S5.1. Crystal Data

Empirical Formula	IrCl <sub>3</sub> O <sub>2</sub> NC <sub>23</sub> H <sub>25</sub>
Formula Weight	646.04
Crystal Color, Habit	yellow, prism
Crystal Dimensions	0.13 X 0.10 X 0.05 mm
Crystal System	monoclinic
Lattice Type	Primitive
Indexing Images	6 images @ 20.0 seconds
Detector Position	49.90 mm
Lattice Parameters	a = 8.2581(8) Å b = 15.3706(14) Å c = 20.2039(18) Å β = 92.606(2)° V = 2561.9(4) Å <sup>3</sup>
Space Group	P2 <sub>1</sub> /n (#14)
Z value	4
D <sub>calc</sub>	1.675 g/cm <sup>3</sup>
F <sub>000</sub>	1256.00
μ(MoKα)	55.566 cm <sup>-1</sup>

### S5.2. Intensity Measurements

Diffractometer	Rigaku SCXmini
Radiation	MoKα (λ = 0.71075 Å)
Detector Aperture	75 mm round
Data Images	540 images
Exposure Rate	60.0 sec./°
ω oscillation Range 1 (χ=54.0, φ=0.0)	-120.0 - 60.0°
ω oscillation Range 1 (χ=54.0, φ=120.0)	-120.0 - 60.0°
ω oscillation Range 1 (χ=54.0, φ=240.0)	-120.0 - 60.0°
Detector Swing Angle	-28.40°
Detector Position	49.90 mm
2θ <sub>max</sub>	55.0°
No. of Reflections Measured	Total: 25141 Unique: 5823 (R <sub>int</sub> = 0.069)
Corrections	Lorentz-polarization, Absorption (trans. factors: 0.482 - 0.757)

### S5.3. Structure Solution and Refinement

Structure Solution	Direct Methods (SIR92)
Refinement	Full-matrix least-squares on F <sup>2</sup>
Function Minimized	Σ w (F <sub>o</sub> <sup>2</sup> - F <sub>c</sub> <sup>2</sup> ) <sup>2</sup>
Least Squares Weights	w = 1 / [ σ <sup>2</sup> (F <sub>o</sub> <sup>2</sup> ) + (0.0337 · P) <sup>2</sup> + 2.3179 · P ] where P = (Max(F <sub>o</sub> <sup>2</sup> , 0) + 2F <sub>c</sub> <sup>2</sup> )/3
2θ <sub>max</sub> cutoff	55.0°
Anomalous Dispersion	All non-hydrogen atoms
No. Observations (All reflections)	5823
No. Variables	281
Reflection/Parameter Ratio	20.72
Residuals: R1 (I > 2.00σ(I))	0.0469
Residuals: R (All reflections)	0.0783
Residuals: wR2 (All reflections)	0.0900
Goodness of Fit Indicator	1.068
Max Shift/Error in Final Cycle	0.001
Maximum peak in Final Diff. Map	0.87 e <sup>-</sup> /Å <sup>3</sup>
Minimum peak in Final Diff. Map	-0.68 e <sup>-</sup> /Å <sup>3</sup>

## S5.4. Experimental Details

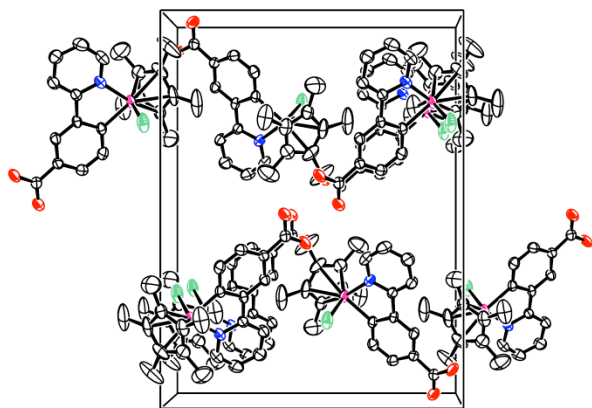
The crystal sample was mounted in a MiTeGen polyimide loop with immersion oil. All measurements were made on a Rigaku Mercury2 CCD area detector with filtered Mo-K $\alpha$  radiation at a temperature of -50°C. The structure was solved by direct methods<sup>8</sup> and expanded using Fourier techniques.<sup>9</sup> The non-hydrogen atoms were refined anisotropically. Hydrogen atoms were refined using the riding model. Chlorine atom Cl2 was refined as occupied over two sites of 0.65 and 0.35 occupancy. Cl2 and Cl2' were restrained to have similar thermal parameters using the SADI restraint. Hydrogen atoms H23A and H23B were added as a riding contribution on the higher occupied of the two methylene chloride orientations. The final cycle of full-matrix least-squares refinement (Least Squares function minimized: (SHELXL97)  $\sum w(F_o^2 - F_c^2)^2$  where  $w = 1/(\sigma^2(F_o^2) + (0.00149P)^2)$  on  $F^2$  was based on 5823 observed reflections and 281 variable parameters and converged (largest parameter shift was 0.00 times its esd) with unweighted and weighted agreement factors of:

$$R1 = \sum ||F_o| - |F_c|| / \sum |F_o| = 0.0469$$
$$wR2 = [ \sum ( w (F_o^2 - F_c^2)^2 ) / \sum w(F_o^2)^2 ]^{1/2} = 0.0900$$

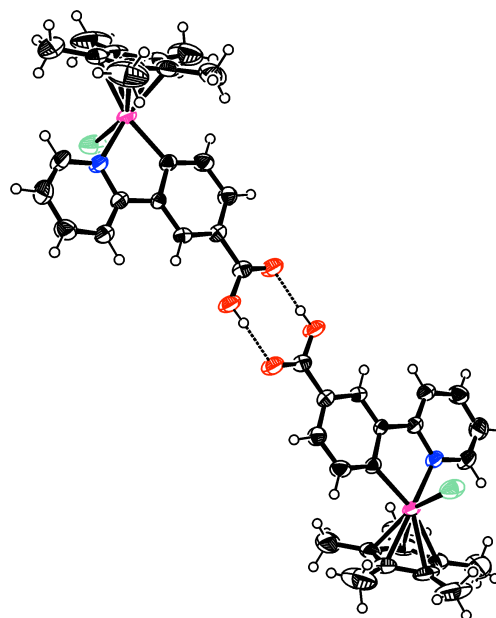
The standard deviation of an observation of unit weight (Standard deviation of an observation of unit weight:  $[\sum w(F_o^2 - F_c^2)^2 / (No - Nv)]^{1/2}$  where: No = number of observations, Nv = number of variables) was 1.07. Unit weights were used. The maximum and minimum peaks on the final difference Fourier map corresponded to 0.87 and -0.68 e<sup>-</sup>/Å<sup>3</sup>, respectively.

Neutral atom scattering factors were taken from Cromer and Waber.<sup>10</sup> Anomalous dispersion effects were included in Fcalc<sup>11</sup>; the values for  $\Delta f'$  and  $\Delta f''$  were those of Creagh and McAuley.<sup>12</sup> The values for the mass attenuation coefficients are those of Creagh and Hubbell.<sup>13</sup> All calculations were performed using the CrystalStructure<sup>14</sup> crystallographic software package except for refinement, which was performed using SHELXL-97.

## S5.5. Additional Images



View of packing along a  
(H-atoms and solvent omitted)



View of H-bond pair

**Table S1.** Atomic coordinates and  $B_{\text{iso}}/B_{\text{eq}}$

atom	x	y	z	$B_{\text{eq}}^a$
Ir(1)	0.43025(3)	0.601813(14)	0.271956(12)	2.836(7)
Cl(1)	0.6563(2)	0.54669(11)	0.21413(10)	4.83(4)
Cl(2)	0.8433(13)	0.1166(8)	0.5078(4)	20.9(4)
Cl(2')	0.655(5)	0.078(2)	0.4856(13)	35.6(17)
Cl(3)	0.6043(8)	0.2189(6)	0.4340(3)	25.8(3)
O(1)	0.5716(5)	0.9737(2)	0.0840(2)	4.11(9)
O(2)	0.3900(5)	0.9130(2)	0.0130(2)	3.93(9)
N(1)	0.5936(5)	0.6910(3)	0.3162(2)	2.98(9)
C(1)	0.3594(8)	0.5106(5)	0.3529(4)	4.88(17)
C(2)	0.3339(9)	0.4681(4)	0.2904(4)	4.94(17)
C(3)	0.2223(8)	0.5191(4)	0.2504(3)	3.94(13)
C(4)	0.1739(7)	0.5913(4)	0.2890(3)	4.09(14)
C(5)	0.2638(9)	0.5875(4)	0.3510(3)	4.52(15)
C(6)	0.4643(11)	0.4735(7)	0.4089(5)	9.9(3)
C(7)	0.4090(11)	0.3849(4)	0.2690(5)	9.0(3)
C(8)	0.1473(11)	0.4918(6)	0.1845(4)	8.0(2)
C(9)	0.0425(9)	0.6564(5)	0.2678(5)	7.2(2)
C(10)	0.2472(12)	0.6507(6)	0.4069(4)	8.2(2)
C(11)	0.6791(8)	0.6778(4)	0.3741(3)	3.96(13)
C(12)	0.7775(8)	0.7386(4)	0.4029(3)	4.32(14)
C(13)	0.7941(8)	0.8183(4)	0.3723(3)	3.98(13)
C(14)	0.7140(7)	0.8328(3)	0.3114(3)	3.30(12)
C(15)	0.6138(6)	0.7681(3)	0.2845(2)	2.55(10)
C(16)	0.5228(6)	0.7734(3)	0.2202(2)	2.33(9)
C(17)	0.5359(7)	0.8430(3)	0.1766(2)	2.74(10)
C(18)	0.4476(7)	0.8425(3)	0.1160(2)	2.59(10)
C(19)	0.3456(7)	0.7721(3)	0.1007(2)	3.16(11)
C(20)	0.3354(7)	0.7026(3)	0.1434(3)	3.49(12)
C(21)	0.4215(6)	0.7006(3)	0.2045(2)	2.48(9)
C(22)	0.4661(7)	0.9127(3)	0.0668(3)	2.87(10)
C(23)	0.7582(18)	0.1575(15)	0.4391(8)	16.0(6)

**Table S2.** Atomic coordinates and  $B_{\text{iso}}$  of hydrogen atoms

atom	x	y	z	$B_{\text{iso}}$
H(1A)	0.5812	1.0081	0.0527	4.95
H(23A)	0.8443	0.1892	0.4176	19.24
H(23B)	0.7315	0.1075	0.4105	19.24
H(6A)	0.5112	0.4190	0.3950	11.83
H(6B)	0.3990	0.4634	0.4469	11.83
H(6C)	0.5503	0.5143	0.4209	11.83
H(7A)	0.5251	0.3926	0.2665	10.86
H(7B)	0.3630	0.3685	0.2257	10.86
H(7C)	0.3874	0.3395	0.3007	10.86
H(8A)	0.0664	0.5342	0.1698	9.58
H(8B)	0.0963	0.4353	0.1888	9.58
H(8C)	0.2306	0.4881	0.1523	9.58
H(9A)	0.0316	0.6994	0.3024	8.69
H(9B)	-0.0598	0.6261	0.2602	8.69
H(9C)	0.0718	0.6850	0.2273	8.69
H(10A)	0.3221	0.6351	0.4433	9.83
H(10B)	0.1372	0.6490	0.4217	9.83
H(10C)	0.2716	0.7090	0.3917	9.83
H(11)	0.6695	0.6238	0.3953	4.75
H(12)	0.8341	0.7267	0.4433	5.18
H(13)	0.8588	0.8620	0.3924	4.77
H(14)	0.7274	0.8856	0.2888	3.96
H(17)	0.6040	0.8902	0.1879	3.28
H(19)	0.2830	0.7722	0.0606	3.79
H(20)	0.2687	0.6553	0.1310	4.19

$$^a B_{\text{eq}} = 8/3 \pi^2 (U_{11}(\text{aa}^*)^2 + U_{22}(\text{bb}^*)^2 + U_{33}(\text{cc}^*)^2 + 2U_{12}(\text{aa}^*\text{bb}^*)\cos \gamma + 2U_{13}(\text{aa}^*\text{cc}^*)\cos \beta + 2U_{23}(\text{bb}^*\text{cc}^*)\cos \alpha)$$

**Table S3.** Anisotropic displacement parameters<sup>b</sup>

atom	U <sub>11</sub>	U <sub>22</sub>	U <sub>33</sub>	U <sub>12</sub>	U <sub>13</sub>	U <sub>23</sub>	Occupancy
Ir(1)	0.03848(14)	0.02497(12)	0.04496(15)	-0.00100(12)	0.00925(10)	0.00848(11)	
Cl(1)	0.0576(11)	0.0343(8)	0.0945(14)	0.0068(7)	0.0347(10)	0.0054(8)	
Cl(2)	0.239(10)	0.390(14)	0.156(6)	-0.006(9)	-0.074(7)	0.026(7)	0.654
Cl(2')	0.56(5)	0.54(4)	0.24(2)	-0.24(4)	-0.00(2)	0.16(2)	0.346
Cl(3)	0.226(6)	0.450(11)	0.296(7)	0.140(7)	-0.082(5)	-0.152(8)	
O(1)	0.071(3)	0.041(2)	0.042(2)	-0.019(2)	-0.012(2)	0.017(2)	
O(2)	0.067(3)	0.040(2)	0.042(2)	-0.012(2)	-0.003(2)	0.0107(19)	
N(1)	0.042(2)	0.034(2)	0.037(2)	-0.000(2)	0.004(2)	0.010(2)	
C(1)	0.046(4)	0.073(5)	0.067(5)	-0.021(4)	0.002(3)	0.037(4)	
C(2)	0.057(4)	0.028(3)	0.106(6)	-0.007(3)	0.038(4)	0.013(3)	
C(3)	0.056(4)	0.040(3)	0.055(4)	-0.019(3)	0.007(3)	0.003(3)	
C(4)	0.038(3)	0.044(4)	0.074(5)	-0.009(3)	0.017(3)	0.009(3)	
C(5)	0.062(4)	0.054(4)	0.058(4)	-0.016(3)	0.027(3)	-0.003(3)	
C(6)	0.092(7)	0.157(10)	0.123(8)	-0.043(7)	-0.021(6)	0.103(8)	
C(7)	0.115(8)	0.034(4)	0.202(12)	-0.012(4)	0.084(8)	0.002(5)	
C(8)	0.111(8)	0.113(7)	0.079(6)	-0.067(6)	-0.004(5)	-0.003(5)	
C(9)	0.041(4)	0.064(5)	0.172(10)	0.001(4)	0.020(5)	0.020(6)	
C(10)	0.114(8)	0.122(8)	0.079(6)	-0.052(7)	0.046(6)	-0.030(6)	
C(11)	0.058(4)	0.044(3)	0.048(4)	0.003(3)	0.001(3)	0.020(3)	
C(12)	0.057(4)	0.064(4)	0.042(3)	0.001(3)	-0.007(3)	0.011(3)	
C(13)	0.053(4)	0.050(4)	0.047(3)	-0.013(3)	-0.006(3)	-0.001(3)	
C(14)	0.046(3)	0.037(3)	0.042(3)	-0.005(2)	-0.002(3)	0.009(2)	
C(15)	0.035(3)	0.029(2)	0.033(3)	0.003(2)	0.006(2)	0.004(2)	
C(16)	0.027(3)	0.022(2)	0.039(3)	0.004(2)	0.001(2)	0.004(2)	
C(17)	0.036(3)	0.028(2)	0.040(3)	-0.006(2)	0.001(2)	0.004(2)	
C(18)	0.039(3)	0.028(2)	0.031(3)	0.003(2)	0.005(2)	0.002(2)	
C(19)	0.046(3)	0.041(3)	0.032(3)	-0.004(2)	-0.002(2)	0.002(2)	
C(20)	0.050(4)	0.034(3)	0.048(3)	-0.012(3)	-0.004(3)	-0.003(2)	
C(21)	0.032(3)	0.024(2)	0.038(3)	0.004(2)	0.007(2)	0.002(2)	
C(22)	0.043(3)	0.030(3)	0.036(3)	-0.003(2)	0.004(2)	0.000(2)	
C(23)	0.109(11)	0.34(2)	0.165(15)	0.010(15)	0.016(11)	0.004(16)	

<sup>b</sup> The general temperature factor expression:  $\exp(-2\pi^2(a^2U_{11}h^2 + b^2U_{22}k^2 + c^2U_{33}l^2 + 2a*b*U_{12}hk + 2a*c*U_{13}hl + 2b*c*U_{23}kl))$

**Table S4.** Bond lengths (Å)

atom	atom	distance	atom	atom	distance
Ir(1)	Cl(1)	2.4011(19)	Ir(1)	N(1)	2.094(4)
Ir(1)	C(1)	2.253(8)	Ir(1)	C(2)	2.241(6)
Ir(1)	C(3)	2.165(6)	Ir(1)	C(4)	2.166(6)
Ir(1)	C(5)	2.165(7)	Ir(1)	C(21)	2.040(5)
Cl(2)	C(23)	1.653(19)	O(1)	C(22)	1.315(7)
O(2)	C(22)	1.231(7)	N(1)	C(11)	1.353(7)
N(1)	C(15)	1.361(7)	C(1)	C(2)	1.429(11)
C(1)	C(5)	1.421(10)	C(1)	C(6)	1.505(12)
C(2)	C(3)	1.432(10)	C(2)	C(7)	1.495(10)
C(3)	C(4)	1.425(9)	C(3)	C(8)	1.503(11)
C(4)	C(5)	1.428(10)	C(4)	C(9)	1.523(10)
C(5)	C(10)	1.500(12)	C(11)	C(12)	1.353(9)
C(12)	C(13)	1.381(9)	C(13)	C(14)	1.388(8)
C(14)	C(15)	1.389(8)	C(15)	C(16)	1.473(7)
C(16)	C(17)	1.394(7)	C(16)	C(21)	1.424(7)
C(17)	C(18)	1.395(7)	C(18)	C(19)	1.398(8)
C(18)	C(22)	1.481(7)	C(19)	C(20)	1.378(8)
C(20)	C(21)	1.397(8)			

## S.6. References:

1. G. Li, C. P. Richter, R. L. Milot, L. Cai, C. A. Schmuttenmaer, R. H. Crabtree, G. W. Brudvig and V. S. Batista, *Dalton Transactions*, 2009, 10078-10085.
  2. D. T. Sawyer, A. Sobkowiak and J. L. Roberts, *Electrochemistry for Chemists*, 2nd edn., Wiley, New York, 1995.
  3. A. J. Bard and L. R. Faulkner, *Electrochemical Methods: Fundamentals and Applications*, 2nd edn., Hoboken, 2001.
  4. M. C. Beard, G. M. Turner and C. A. Schmuttenmaer, *Physical Review B: Condensed Matter and Materials Physics*, 2000, 62, 15764-15777.
  5. J. B. Baxter and C. A. Schmuttenmaer, *Journal of Physical Chemistry B*, 2006, 110, 25229-25239.
  6. G. M. Turner, M. C. Beard and C. A. Schmuttenmaer, *Journal of Physical Chemistry B*, 2002, 106, 11716-11719.
  7. C.-H. Lee and J. S. Lindsey, *Tetrahedron* 1994, 50, 11427-11440.
  8. G. M. Sheldrick, *Acta Cryst.*, 2008, A64, 112-122.
  9. P. T. Beurskens, G. Admiraal, G. Beurskens, W. P. Bosman, R. de Gelder, R. Israel and J. M. M. T. Smits, *The DIRDIF-99 program system*, University of Nijmegen, The Netherlands, 1999.
  10. D. T. Cromer and J. T. Waber, The Kynoch Press, Birmingham, England, 1974, Table 2.2 A.
  11. J. A. Ibers and W. C. Hamilton, *Acta Cryst.*, 1964, 17, 781.
  12. D. C. Creagh and W. J. McAuley, Kluwer Academic Publishers, Boston, 1992, Table 4.2.6.8, pages 219-222.
  13. D. C. Creagh and J. H. Hubbell, Kluwer Academic Publishers, Boston, 1992, Table 4.2.4.3, pages 200-206.
  14. *CrystalStructure 3.8: Crystal Structure Analysis Package*, (2000-2007) Rigaku Rigaku Americas 9009 New Trails Dr. The Woodlands TX 77381 USA.
-